Synthesis and Characterization of Pd(0) and Pt(0) Metallocryptands Encapsulating Tl^+ Ion

Vincent J. Catalano,*,† Byron L. Bennett,†,§ Renante L. Yson,† and Bruce C. Noll‡

Contribution from the Department of Chemistry, University of Nevada, Reno, Nevada 89557, and Department of Chemistry and Biochemistry, University of Colorado, Boulder, Colorado 80309

Received May 15, 2000

Abstract: Pt(0)/Pd(0) metallocryptates encapsulating Tl(I) have been constructed utilizing mixed phosphine-imine ligands 2,9-bis(diphenylphosphino)-1,10-phenathroline, P_2phen, and 6,6′-bis(diphenylphosphino)-2,2′-bipyridine, P_2bpy. The red compounds $[M_2Tl(P_2phen)_3](NO_3)$ (M = Pt, **1**; M = Pd, **3**) and $[M_2Tl(P_2bpy)_3](NO_3)$ (M = Pt, **2**; M = Pd, **4**) have been isolated as air-stable crystalline solids. Complexes **1**−**4** exhibit single signals in their ^{205}Tl NMR spectra that are well deshielded compared to the $TlNO_{3(aq)}$ reference signal. Additionally, ^{195}Pt NMR spectra of complexes **1** and **2** exhibit a doublet of quartets pattern resulting from large one-bond couplings to both ^{31}P and ^{205}Tl. Characterization of **1**−**4** by single-crystal X-ray diffraction studies confirms the metallocryptand structure consisting of three phosphine-imine ligands in a D_3-symmetric cage with the Tl(I) ion in its center and the zero-valent Pt or Pd atoms on each end. Each Pd or Pt atom is coordinated to three phosphorus centers, forming approximately trigonal geometry. The Tl(I) ion is positioned away from the imine nitrogen atoms of the phosphine ligands by ∼3.5 Å. Further, the outer capping metals are distorted toward the central Tl(I) ion, indicating a strong interaction. The Pt−Tl and Pd−Tl separations are at ∼2.8 Å each, further manifesting the strength of the metallophilic attraction in these assemblies.

Introduction

Metallocryptates are an emerging class of inorganic cage complexes that are well-suited to encapsulate a variety of metal ions.[1,2,4] Unlike their purely organic counterparts, metallocryptates are capable of binding metal ions either through strong Lewis base interactions of the donor groups of the ligands or through metallophilic interactions between the late transition metal capping groups and the guest metal ion. In the absence of attractive guest−ligand interactions, metallocryptates offer a unique opportunity to explore the remaining metal−metal interactions in a rigidly controlled environment.

Recently, we reported the syntheses of cationic Au(I)-based metallocryptates,[2] $[Au_2M(P_2phen)_3]^{3+}$ (M = Na^+ and Tl^+; P_2-phen = 2,9-bis(diphenylphosphino)-1,10-phenathroline,[3] **A** in Chart1). Each species contains Au centers in trigonal coordination environments, a D_3-symmetrical cavity imposed by helical phenanthroline subunits, long guest ion−imine distances, and a nearly linear Au−M−Au core. In $[Au_2Tl(P_2phen)_3]^{3+}$, two short Au(I)−Tl(I) distances of ∼2.9 Å are observed, indicative of a strong interaction between these two closed-shell ions. However, replacing the aurophilic Tl(I) ion with a Na^+ ion eliminates the metallophilic interaction, making this assembly unstable, and the alkali metal readily dissociates. In contrast, by employing the 2,9-bis(diphenylphosphino)-1,8-naphthyridine ligand (dppn) which is capable of strong imine−Na^+ interactions, the assembly is maintained (**B** in Chart 1).[4] In fact, Na^+ is preferred over Tl(I) ion in this case.

Chart 1

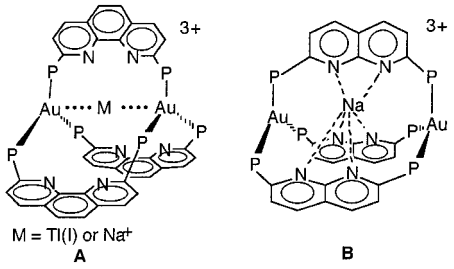

This aurophilic and metallophilic behavior between formally closed-shell ions and atoms has been invoked previously[5] and theoretically treated.[6] There is a considerable attraction between closed-shell species, and a large number of inorganic assemblies based on this attraction have been reported.[7] In many cases it is difficult to separate purely metallophilic interactions from secondary ligand interactions. However, metallocryptands, with

* To whom correspondence should be addressed. E-mail: VJC@unr.edu. Fax: (775) 784-6804.

† University of Nevada, Reno.

‡ University of Colorado, Boulder.

§ Current address: Department of Chemistry, University of Nevada, Las Vegas, NV 89154.

(1) Uang, R.-H.; Chan, C.-K.; Peng, S.-M.; Che, C.-M. *J. Chem. Soc., Chem. Commun.* **1994**, 2561.

(2) Catalano, V. J.; Bennett, B. B.; Kar, H. M.; Noll, B. C. *J. Am. Chem. Soc.* **1999**, *121*, 10235.

(3) Ziessel, R. *Tetrahedron Lett.* **1989**, *30*, 463.

(4) Catalano, V. J.; Kar, H. M.; Bennett, B. L. *Inorg. Chem.* **2000**, *39*, 121.

(5) (a) Fernández, E. J.; López-de-Luzuriaga, J. M.; Monge, M.; Rodríguez, M. A.; Crespo, O.; Gimeno, M. C.; Laguna, A.; Jones, P. G. *Chem. Eur. J.* **2000**, *6*, 636. (b) Pyykkö, P.; Runeberg, N.; Mendizabal, F. *Chem. Eur. J.* **1997**, *3*, 1451. (c) Pyykkö, P.; Mendizabal, F. *Inorg. Chem.* **1998**, *37*, 3018. (d) Fernández, E. J.; López-de-Luzuriaga, J. M.; Monge, M.; Rodríguez, M. A.; Crespo, O.; Gimeno, M. C.; Laguna, A.; Jones, P. G. *Inorg. Chem.* **1998**, *37*, 6002. (e) Schmidbaur, H. *Chem. Soc. Rev.* **1995**, 391.

(6) Pyykkö, P. *Chem. Rev.* **1997**, *97*, 597.

(7) (a) Crespo, O.; Fernandez, E. J.; Jones, P. G.; Laguna, A.; Lopez-de-Luzuriaga, J. M.; Mendia, A.; Monge, M.; Olmos, E. *J. Chem. Soc., Chem. Commun*. **1998**, 2233. (b) Wang, S.; Garzón, G.; King, C.; Wang, J.-C.; Fackler, J. P., Jr. *Inorg. Chem.* **1989**, *28*, 4623. (c) Wang, S.; Fackler, J. P., Jr.; King, C.; Wang, J. C. *J. Am. Chem. Soc.* **1988**, *110*, 3308.

10.1021/ja001672s CCC: $19.00
Published on Web 09/22/2000

Scheme 1

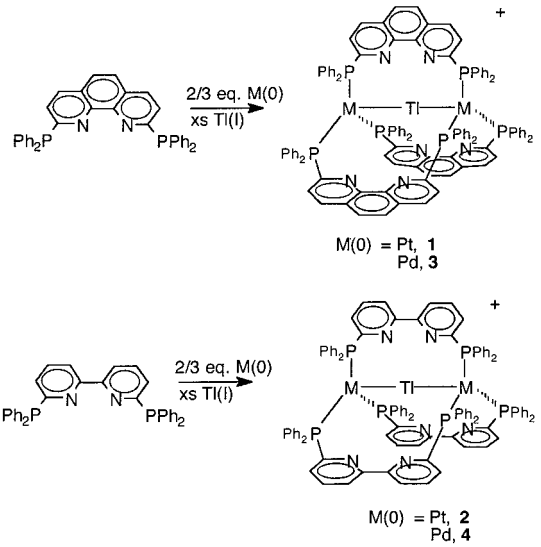

Table 1. NMR Data for Complexes **1**−**4**

complex	$^{31}P\{^1H\}\delta$	$^{205}Tl\ \delta$	$^{195}Pt\ \delta$	observed couplings (Hz)
$[Pt_2Tl(P_2phen)_3](NO_3)$, **1**	+46.1[a]	+1866[b]	−4119[c]	^1J(Tl−Pt) = 5560 ^1J(Pt−P) = 4436
$[Pt_2Tl(P_2bpy)_3](NO_3)$, **2**	+35.3[a]	+2390[b]	−4120[c]	^1J(Tl−Pt) = 6100 ^1J(Pt−P) = 4332
$[Pd_2Tl(P_2phen)_3](NO_3)$, **3**	+27.1[d]	+2022[e]		
$[Pd_2Tl(P_2bpy)_3](NO_3)$, **4**	+21.6[d]	+2636[e]		

[a] 121 MHz, 25 °C, $CDCl_3$. [b] 288.8 MHz, 25 °C, DMSO, external reference $Tl(NO_3)_{(aq)}$. [c] 107.0 MHz, 25 °C, DMSO/$CDCl_3$, external reference $H_2PtCl_{6(aq)}$. [d] 121 MHz, 25 °C, $CDCl_3/CD_3CN$. [e] 288.8 MHz, 25 °C, CD_3CN, external reference $Tl(NO_3)_{(aq)}$.

their large cavities, provide a convenient means to study the guest−metal attractions in the absence of guest−ligand interactions. Herein we report the synthesis and characterization of Pt(0)- and Pd(0)-based metallocryptands with encapsulated Tl(I) ion.

Results

The metallocryptate complex $[Pt_2Tl(P_2phen)_3](NO_3)$, **1**, was prepared by addition of $Pt(dba)_2$ (dba = dibenzylideneacetone) to a dichloromethane solution of the P_2phen ligand containing excess $TlNO_3$ (Scheme 1). Analogously, the Pd-containing congener, $[Pd_2Tl(P_2phen)_3](NO_3)$, **3**, is synthesized using $Pd_2(dba)_3{\cdot}CHCl_3$. Alternatively, utilization of 6,6′-bis(diphenylphosphino)-2,2′-bipyridine, P_2bpy, in place of P_2phen readily yields $[Pt_2Tl(P_2bpy)_3](NO_3)$, **2**, and $[Pd_2Tl(P_2bpy)_3](NO_3)$, **4**. The nitrate salts of **1**−**4** were isolated as red-orange solids. Additionally, $Pt(AsPh_3)_4$[8] may be used in place of $Pt(dba)_2$, producing similar results. Compounds **1**−**4** are all moderately soluble in dichloromethane, 1,2-dichloroethane, acetonitrile, tetrahydrofuran, and acetone, moderately soluble in alcohols, and practically insoluble in diethyl ether, benzene, or toluene. Solutions are stable to air and moisture for several days.

Solution-state NMR spectroscopy supports the proposed structural formulations of **1**−**4** (Table 1). ^{205}Tl spectra of **1**−**4** display broad single resonances with chemical shifts well downfield from typical thallium(I) signals.[9] Complexes **1** and **2** exhibit nearly identical ^{195}Pt spectra consisting of a doublet

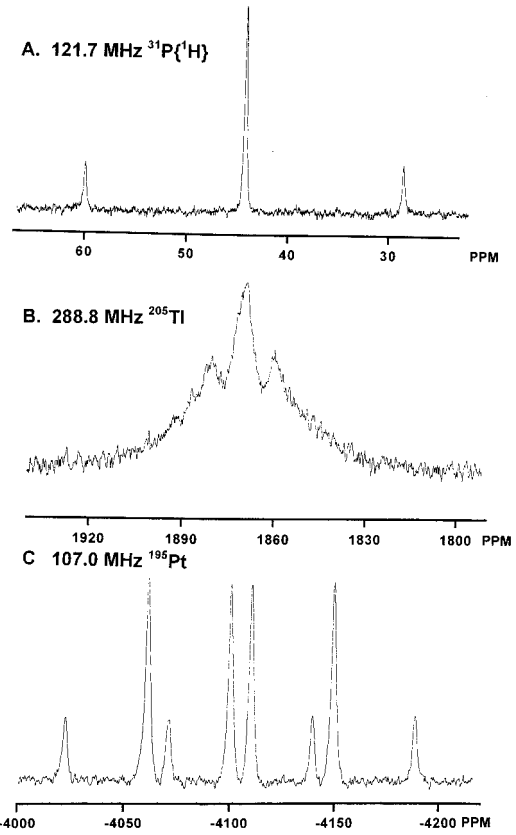

Figure 1. (A) 121.7-MHz $^{31}P\{^1H\}$ NMR spectrum of **1** in CD_3CN at 25 °C, showing coupling to ^{195}Pt ($I = 1/2$, 33% abundant) but not to ^{203}Tl or ^{205}Tl. (B) 288.8-MHz ^{205}Tl NMR spectrum displaying the anticipated five-line pattern for the statistical mixture of isotopomers (outer two lines are obscured in the noise). A $^1J(^{205}Tl-Pt)$ coupling is observed. (C) 107.0-MHz ^{195}Pt NMR spectrum showing ^1J(Pt−Tl) = 5560 and ^1J(Pt−P) = 4436 Hz.

of quartets, confirming coupling to three equivalent ^{31}P nuclei and a single Tl nucleus (^{195}Pt 33.8% abundant, $I = 1/2$; ^{203}Tl 29.5% abundant, $I = 1/2$; ^{205}Tl 70.5% abundant, $I = 1/2$). Because of the large line widths and nearly identical gyromagnetic ratios, the individual couplings to ^{203}Tl and ^{205}Tl could not be differentiated. The ^{195}Pt chemical shifts observed for **1** and **2** are typical of three-coordinate Pt(0) and slightly deshielded in comparison to the $Pt(PPh_3)_3$ shift (−4583 ppm).[10] The $^{31}P\{^1H\}$, ^{205}Tl, and the ^{195}Pt NMR spectra of **1** are shown in Figure 1.

The observation of sharp, single $^{31}P\{^1H\}$ resonances for species **1**−**4** supports the highly symmetrical environment of the metallocryptate complex (Table 1). The chemical shifts of **1**−**4** compare well with the related species $Pd(PPh_3)_3$ (22.6 ppm)[10] and $Pt(PPh_3)_3$ (49.9 ppm).[11] Additionally, the $^{31}P\{^1H\}$ signals for **1** and **2** exhibit typical couplings to ^{195}Pt as compared to $Pt(PPh_3)_3$ (^1J(Pt−P) = 4455 Hz).[10] Interestingly, no coupling of ^{31}P to Tl is observed (line width < 10 Hz) for **1**−**4**. This is in contrast to the 186 Hz ^2J(P−Tl) observed in the analogous $[Au_2Tl(P_2phen)_3]^{3+}$ complex.[2]

Proton NMR spectra further support the highly symmetrical character of **1**−**4** by displaying single signals for the three magnetically distinct phenanthroline and bipyridine protons. These signals are only minimally shifted (±0.06 ppm) relative to those of the respective uncoordinated ligands. However, two sets of resonances corresponding to phenyl ring protons are

(8) Malatesta, L.; Cariello, C. *J. Chem. Soc.* **1958**, 2323.
(9) Brevard, C.; Granger, P. *Handbook of High-Resolution Multinuclear NMR*; Wiley-Interscience: New York, 1981.
(10) Mann, B. E.; Musco, A. *J. Chem. Soc., Dalton Trans.* **1975**, 1673.
(11) Benn, R.; Buech, H. M.; Reinhardt, R. *Magn. Reson. Chem.* **1985**, *23*, 559.

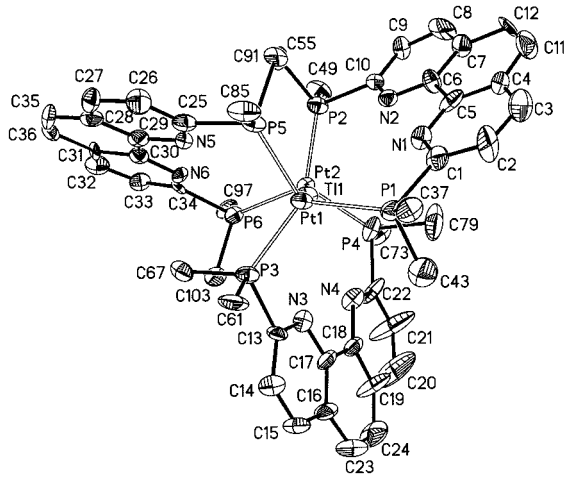

Figure 2. X-ray structural drawing for the cation of **1** viewed looking down the metal−metal axis. Hydrogen atoms and all but the ipso carbon of the phenyl rings are omitted for clarity.

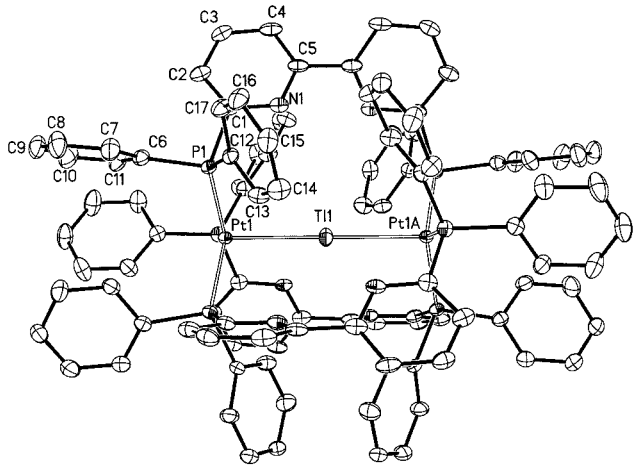

Figure 3. Thermal ellipsoid plot of **2** with hydrogen atoms omitted for clarity, emphasizing the two phenyl ring environments, parallel and perpendicular to the metal−metal axis. Only the asymmetric unit and the metals are numbered. The Tl atom resides on a three-, two-fold crystallographic symmetry element.

observed in the metallocryptates. Interpretation of the ^{31}P-selective and homonuclear decoupling experiments suggests that two phenyl ring environments exist: one along the metal−metal axis and one equatorial to this axis (vide supra). Variable-temperature experiments in CD_3CN up to 70 °C reveal no exchange processes between the two ring environments. This lack of interchange suggests that the helical nature of these complexes is maintained in solution, as there is no evidence of a trigonal twisting process that would interconvert the M and P helices.

Complexes **1** and **3** were additionally characterized in the gas phase by MALDI-TOF and FAB mass spectrometry (nitrobenzyl alcohol matrix, Supporting Information). For such large molecules there is remarkably little fragmentation. The mass spectra for both compounds contain peaks assigned to the molecular ion along with peaks corresponding to the loss of one ligand followed by loss of Tl^+ ion. Further, the most intense peak in all of the spectra corresponds to the loss of one ligand while the three-metal core is maintained. The composition of this species is verified by its distinct isotopomer pattern.

In solution, the electronic absorption spectra of complexes **1**−**4** exhibit high-energy features (λ < 320 nm) corresponding to $\pi-\pi^*$ transitions and a single broad intense feature near 450 nm (Experimental Section). No emission out to 800 nm was observed for any the complexes reported here.

The electrochemical character of **1**−**4** was probed by cyclic voltammetry in acetonitrile and dichloromethane. No reversible oxidative features were observed for complexes **1**−**4**; however, reductive processes (quasi-reversible) were observed in the range expected for ligand reductions between −1.0 and −1.6 V.[12] Further, chemical oxidation with I_2 and Br_2 was equally unsuccessful, producing only decomposition and phosphine oxide. No reaction was observed for the addition of CH_3I to **3** with either thermal initiation or photoinitiation. Moreover, the outer metals are not available for further coordination, as no reaction of **3** with triethyl phosphite, pyridine, acetonitrile, or *n*-butyl isonitrile was noted.

The solid-state structures of **1**−**4** were probed by single-crystal X-ray diffraction, and thermal ellipsoid drawings are provided in Figures 2−5, while selected bond distances and angles are tabulated in Table 2. The cationic portions of the molecules are remarkably similar within each ligand set.

(12) Lever, A. B. P. *Inorg. Chem.* **1990**, *29*, 1271.

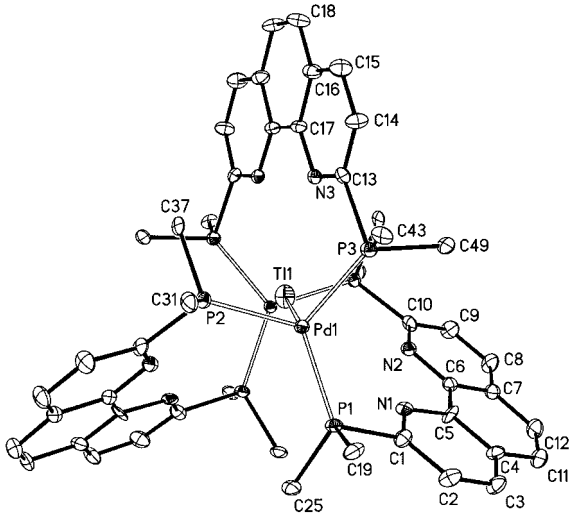

Figure 4. X-ray structural drawing for the cation of **3** viewed end-on, emphasizing the helical nature of the cation. Only the asymmetric unit is numbered. The Tl atom resides on a crystallographic two-fold symmetry element. Hydrogen atoms and all but the ipso carbon of the phenyl rings are omitted for clarity.

Compounds **1** and **3** crystallize in the monoclinic space group *C*2/*c*; however, in **3** only half of the cation is crystallographically unique (related by a two-fold axis), while in **1** the entire cation is crystallographically unique. Compounds **2** and **4** are isostructural and crystallize in the rhombohedral space group $R\bar{3}c$.

The trimetallic cores of molecules **1**−**4** are nearly linear, with an average M−Tl−M angle of 174°. The metal−metal separations are short and reside near the sum of the covalent radii. For **1** and **2**, the Pt−Tl separations are nearly equal, with Pt(1)−Tl(1) and Pt(2)−Tl(1) distances of 2.7907(9) and 2.7919(9) Å, respectively, for **1** and a Pt(1)−Tl(1) distance of 2.7953(2) Å for **2**. Similarly, for **3** and **4** the Pd(1)−Tl(1) separations are 2.7914(6) and 2.7678(6) Å, respectively. The coordination geometry about each Pt and Pd center is roughly trigonal, with a slight displacement of Pt and Pd out of the trigonal plane (0.3507 Å average) toward the Tl atom. In **2**, the P−M−P angles are equal at 117.68(1)°, and in **4** they are 117.44(2)°. In the corresponding P_2phen species, the angles are different, with P(1)−Pd−P(3), P(1)−Pd−P(5), and P(3)−Pd−P(5) angles of

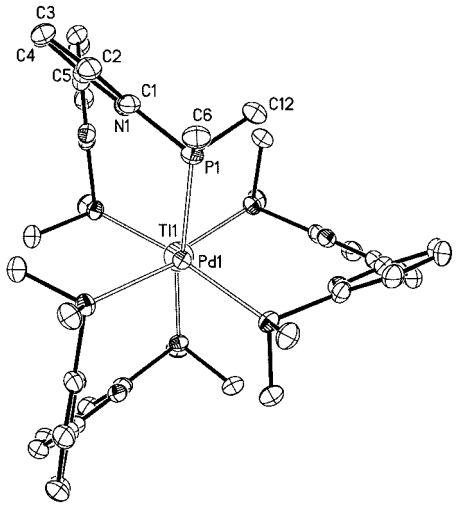

Figure 5. Thermal ellipsoid drawing for the cation of **4** viewed end-on, emphasizing the three-fold symmetry and the helical nature of the cation. Hydrogen atoms and all but the ipso carbon of the phenyl rings are omitted for clarity. Only the asymmetric unit is numbered. The Tl atom resides on a three-, two-fold crystallographic symmetry element.

119.0(1), 124.5(1), and 111.4(1)° for **1** and 120.62(3), 122.40(7), and 110.02(7)° for **2**. These angles are similar to those found in the structure of $Pt(PPh_3)_3$ that shows two angles of 122° and one contracted to 115°.[13] The deviation of trigonal planarity is reflected in the obtuse P−M−Tl angles observed in **1** (97.86° average) and **2** (98.83°) for the Pt complexes and in **3** (98.51° average) and **4** (99.29°) for the Pd complexes.

As seen in Figures 2−5, all of the complexes are helical, but as dictated by the crystallography the bulk material is racemic. The helical nature of the cation is manifested in the phenanthroline portions of **1** and **3** with the three "propeller blade" features, affording an overall D_3 symmetry. Cations **2** and **4** also exhibit D_3 symmetry along with rotation around the 2−2′ carbon−carbon bonds of each bipyridine (dihedral angle = 47°), allowing the two sets of phosphorus atoms to achieve a "staggered" configuration. Two separate orientations of the phenyl rings attached to phosphorus atoms are evident. The $P-C_{ipso}$ bond describes a vector for each phenyl ring environment: one is almost parallel to the metal−metal axis, while the other is orthogonal.

Discussion

The compounds reported here represent new examples of a growing class of inorganic cage complexes called metallocryptands that, in the absence of strong guest−ligand attractions, utilize strong metallophilic interactions to maintain their assembly. This concept is exemplified by comparing the Au(I)-dppn metallocryptates to the P_2phen analogues. In the latter complexes there are no Tl(I)−ligand interactions, and the Tl(I) ion is held tightly solely by a strong bonding interaction with the Au(I) ions. In contrast, the dppn metallocryptates possess ligands that allow for attractive ligand−ion interactions and can bind alkali metal ions that have little or no affinity for Au(I) ion. Moreover, it was originally believed that a template synthesis was necessary to form metallocryptates, and efforts to prepare Au(I)-P_2bpy cryptates were unsuccessful, presumably because the flexibility or rotation around the 2−2′ C−C bond precluded template formation. However, the successful synthesis and characterization of **2** and **4** implies that ligand rigidity and the template effect are not stringent requirements for metallocryptate formation.

Compounds **1**−**4** are synthesized easily and are remarkably air-stable. In contrast, $M(PR_3)_3$[14] and $M_2(dppm)_3$[15] (M = Pt or Pd) are air-sensitive both in solution and in the solid state. The encapsulation of thallium has been confirmed by multiple techniques including MALDI-TOF mass spectrometry, elemental analysis, and NMR spectroscopy. In the MALDI-TOF mass spectra, several thallium-containing fragments were identified, demonstrating the high stability of the metal−thallium bonds. In solution, direct observation of ^{205}Tl NMR signals coupled to ^{195}Pt nuclei not only supports Tl ion encapsulation but also indicates substantial interaction. As rationalized by Oro and co-

Table 2. Bond Distances and Angles for **1**−**4**

Distances (Å)

	$[Pt_2Tl(P_2phen)_3]^+$, **1**	$[Pt_2Tl(P_2bpy)_3]^+$, **2**
Pt(1)−Tl(1)	2.7907(9)	2.7953(2)
Pt(2)−Tl(1)	2.7919(9)	
Pt(1)···Pt(2)	5.578(1)	5.591(1)
Pt(1)−P(1)	2.269(5)	2.312(1)
Pt(1)−P(3)	2.284(4)	
Pt(1)−P(5)	2.279(4)	
Pt(2)−P(2)	2.298(4)	
Pt(2)−P(4)	2.277(4)	
Pt(2)−P(6)	2.281(4)	
Tl(1)−N(1)	3.60(2)	3.886(5)
Tl(1)−N(2)	3.63(2)	
Tl(1)−N(3)	3.39(2)	
Tl(1)−N(4)	3.38(2)	
Tl(1)−N(5)	3.69(2)	
Tl(1)−N(6)	3.73(2)	
	$[Pd_2Tl(P_2phen)_3]^+$, **3**	$[Pd_2Tl(P_2bpy)_3]^+$, **4**
Pd(1)−Tl(1)	2.7914(6)	2.7678(6)
Pd(1)···Pd(2)	5.503(2)	5.536(2)
Pd(1)−P(1)	2.3254(2)	2.345(1)
Pd(1)−P(2)	2.326(2)	
Pd(1)−P(3)	2.310(2)	
Tl(1)−N(1)	3.91(1)	3.89(2)
Tl(1)−N(2)	3.76(1)	
Tl(1)−N(3)	3.19(1)	

Angles (deg)

	1	**2**
Pt(1)−Tl(1)−Pt(2)	175.27(3)	180
P(1)−Pt(1)−P(3)	119.00(16)	117.685(14)
P(1)−Pt(1)−P(5)	124.50(16)	
P(3)−Pt(1)−P(5)	111.40(16)	
P(2)−Pt(2)−P(4)	114.42(18)	
P(4)−Pt(2)−P(6)	119.97(17)	
P(2)−Pt(2)−P(6)	119.43(16)	
P(1)−Pt(1)−Tl(1)	97.90(13)	98.83(3)
P(3)−Pt(1)−Tl(1)	95.84(11)	
P(5)−Pt(1)−Tl(1)	98.67(11)	
P(2)−Pt(2)−Tl(1)	97.77(11)	
P(4)−Pt(2)−Tl(1)	95.99(12)	
P(6)−Pt(2)−Tl(1)	101.04(11)	
	3	**4**
Pd(1)−Tl(1)−Pd(2)	160.62(3)	180
P(1)−Pd(1)−P(3)	120.63(7)	117.44(2)
P(1)−Pd(1)−P(2)	122.40(7)	
P(3)−Pd(1)−P(2)	110.02(7)	
P(1)−Pd(1)−Tl(1)	105.51(5)	99.29(4)
P(2)−Pd(1)−Tl(1)	93.88(5)	
P(3)−Pd(1)−Tl(1)	96.16(5)	

(13) Albano, V.; Bellon, P. L.; Scatturin, V. *J. Chem. Soc., Chem. Commun.* **1966**, 507.

(14) Kuran, W.; Musco, A. *Inorg. Chim. Acta* **1975**, *12*, 187.

(15) Caspa, J. V. *J. Am. Chem. Soc.* **1985**, *107*, 6718.

workers[16] with theoretical support by Pyykkö et al.,[17] extreme deshielding of the Tl(I) nucleus may be the result of spin−orbit effects dictated by the heavy atoms with which it interacts. The lack of Tl coupling to ^{31}P in **1**−**4** is puzzling, given the observation of a ^2J(P−Tl) of 186 Hz in the structurally similar $[Au_2Tl(P_2phen)_3]^{3+}$ complex. Since a similar observation is noted in the analogous $[Pd_2Pb(P_2phen)_3]^{2+}$ and $[Pt_2Pb(P_2phen)_3]^{2+}$ complexes,[18] the effect must be related to the inclusion of the zero-valent capping metals. The simplest explanation suggests a diminution of s character in the M(0)−Tl bond in **1**−**4** compared to that in the Au(I) analogue. Simple relativistic arguments[19] suggest that Au(I) would have the smallest d−s gap and hence greater d^9s^1 character than either Pt(0) or Pd(0). This notion has been invoked to describe many of the unusual observations noted in Au(I) chemistry.[20] Moreover, using calculations to describe the bonding of the trigonally coordinated AuP_2S complex, Fackler and co-workers[21] noted a significant decrease in the contribution of the Au 6s orbital in the (metal−ligand bonding) HOMO, concurrent with an increase in the LUMO as compared to the linear AuP_2 system. Such a contribution allows for a greater participation of the Au 6s orbital for metal−metal bonding.

The electronic spectra of complexes **1**−**4** exhibit absorption peaks below 320 nm that are tentatively assigned to ligand-based processes. As expected, these red/orange complexes also absorb in the visible region.[22] The platinum complexes **1** and **2** absorb at lower energy (454 and 469 nm) than their palladium analogues **3** and **4** (424 and 450 nm), reflecting a significant difference in HOMO−LUMO gap as principal quantum number is altered. The trend may be rationalized[23] as an increase in overlap and therefore a decreased HOMO−LUMO gap for the Pt system, as exemplified by the simplified molecular orbital diagram presented in Figure 6.

Unlike other trigonal Pt(0) and Pd(0) systems,[22] the compounds reported here are not intensely photoluminescent in the visible portion of the electromagnetic spectrum. This is curious when compared to the isoelectronic $[Au_2Tl(P_2phen)_3]^{3+}$ species, which is highly emissive. These results are in line with the lack of electrochemical redox behavior noted in **1**−**4** and the resulting inertness of the three-metal assembly.

Although there are many examples describing the association of Pt(II) centers with Tl(I),[24] there are no examples of the corresponding trigonally coordinated, zero-valent Pt or Pd systems with Tl(I) ions. Pt(0)−Tl(I) separations ranging from 2.860(3) to 2.992(3) Å have been reported by Puddephatt and co-workers[25] in a cluster compound that contains Tl(I) bound to the Pt_3^0 triangular face. The metallocrypands described here offer a relatively simple way to probe these metal−metal interactions in the absence of restrictive ligand−Tl(I) ion interactions. All of the four structures exhibit long N−Tl separations, averaging greater than 3.5 Å. When compared with sum of the covalent radii for Tl and N (2.23 Å), these separations indicate little to no interaction. Furthermore, the N−Tl separation is longest for **2** and **4** (3.88 and 3.89 Å), where the pyridyl rings twist, positioning the imine lone pairs without proper directionality for interaction with the Tl atom. The most striking features of **1**−**4** are their short metal−metal separations. All four structures exhibit interatomic separations between the formally closed-shell Pd(0)/Pt(0) atoms and Tl(I) ion which almost match the sum of the appropriate covalent radii (Pt−Tl, 2.78 Å; Pd−Tl, 2.76 Å). The short M(0)−Tl(I) separations of **1**−**4** are close to the analogous separations (2.708(1) and 2.698(1) Å) in $[Tl\{Pt(C_6F_5)_4\}_2]^{2-}$, which formally contains two Pt(II) ions and a Tl(II) ion.[26] In light of the molecular orbital diagram of Figure 6, the metal core of this compound can be viewed as having one fewer electron than **1** or **2** and thus an increased bond order by one-half. The deformation of the Pt and Pd centers toward Tl is another reflection of this strong attraction. This "inward" puckering is noted even in the isoelectronic and cationic Au(I) system, where the positive charges might be expected to repel each other.

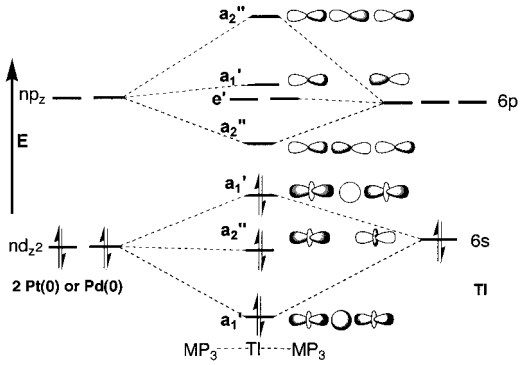

Figure 6. Simplified molecular orbital picture for two trigonally coordinated d^{10} metal ions interacting with a Tl(I) center. Only the filled d_{z^2} and empty p_z are considered on the d^{10} metal.

The role of the Tl atom as a donor to the formally 16-electron Pt(0) and Pd(0) centers may explain the relative inertness observed for these metallocryptate species. The strength of this interaction may be responsible for the substitutionally inert character of the metallocryptate species. Formally, a saturated 18-electron Pt(0) or Pd(0) center would be less likely to undergo oxidative processes or increase its coordination number.

Conclusion

Here, we have reported the synthesis and characterization of a new series of metallocrypates that bind Tl(I) ion in the absence of attractive ligand interactions through metallophilic connections. The cationic species **1**−**4** have been characterized by a variety of methods and have considerable stability. From the solid-state structural data it is apparent that interaction of the

(16) Casado, M. A.; Perez-Torrente, J. J.; Lopez, J. A.; Ciriano, M. A.; Lahoz, F. J.; Oro, L. A. *Inorg. Chem.* **1999**, *38*, 2482.

(17) Kaupp, M.; Malkina, O. L.; Malkin, V.; G.; Pyykkö, P. *Chem. Eur. J.* **1998**, *4*, 118.

(18) Catalano, V. J.; Bennett, B. L.; Noll, B. C. *Chem. Commun.* **2000**, 1413.

(19) (a) Bardaji, M.; Laguna, A. *J. Chem. Educ.* **1999**, *76*, 201. (b) Balasubramanian, K. *Relativistic Effects in Chemistry, Part A*; Wiley-Interscience: New York, 1997.

(20) (a) Schmidbaur, H.; Graf, W.; Müller, G. *Angew. Chem., Int. Ed. Engl.* **1988**, *27*, 417. (b) Görling, A.; Rösch, N.; Ellis, D. E.; Schmidbaur, H. *Inorg. Chem.* **1991**, *30*, 3986. (c) Schmidbaur, H. *Gold Bull.* **1990**, *23*, 11.

(21) Assefa, Z.; Staples, R. J.; Fackler, J. P., Jr. *Inorg. Chem.* **1994**, *33*, 2790.

(22) Harvey, P.; Gray, H. B. *J. Am. Chem. Soc.* **1988**, *110*, 2145.

(23) (a) Mann, K. R.; Grodon, J. G., II.; Gray, H. B. *J. Am. Chem. Soc.* **1975**, *97*, 3553. (b) Mann, K. R.; Lewis, N. S.; Williams, R. M.; Gray, H. G.; Gordon, J. G., II. *Inorg. Chem.* **1978**, *17*, 828. (c) Balch, A. L.; Fossett, L. A.; Olmstead, M. M.; Reedy, P. E., Jr. *Organometallics* **1986**, *5*, 1929. (d) Clodfelter, S. A.; Doede, T. M.; Brennan, B. A.; Nagle, J. K.; Bender, D. P.; Turner, W. A.; LaPunzina, P. M. *J. Am. Chem. Soc.* **1994**, *116*, 11379.

(24) (a) Balch, A. L.; Rowley, S. P. *J. Am. Chem. Soc.* **1990**, *112*, 6139. (b) Balch, A. L.; Fung, E. Y.; Nagle, J. K.; Olmstead, M. M.; Rowley, S. P. *Inorg. Chem.* **1993**, *32*, 3295. (c) Nagle, J. K.; Balch, A. L.; Olmstead, M. M. *J. Am. Chem. Soc.* **1988**, *110*, 319. (d) Renn, O.; Lippert, B.; Mutiainen, I. *Inorg. Chim. Acta* **1993**, *208*, 219.

(25) (a) Hao, L.; Vittal, J. J.; Puddephatt, R. J. *Inorg. Chem.* **1996**, *35*, 269. (b) Hao, L.; Xiao, J.; Vittal, J. J.; Puddephatt, R. J.; Manojlović-Muir, L.; Muir, K.; Torai, A. A. *Inorg. Chem.* **1996**, *35*, 658.

(26) Usón, R.; Forniés, J.; Tomas, M.; Gárde, R. *J. Am. Chem. Soc.* **1995**, *117*, 1837.

metal atoms with one another is the dominant bonding interaction within the metallocryptate cavity. The characterization of complexes **1**−**4** supports the concept of "metallophilic" behavior as a fundamental component of bonding in closed-shell systems. These materials may ultimately serve as prototypical systems for detection of closed-shell ions.

Experimental Section

General. Solvents were distilled just prior to use from the appropriate drying agents: CH_2Cl_2 (CaH_2), THF (Na/benzophenone), and acetonitrile (CaH_2). Commercially available reagents included diphenylphosphine (Strem, 10% w/w in hexanes), Ph_3As (Strem), dibenzylideneacetone (Aldrich), K_2PtCl_4 (Pressure Chemical), K_2PdCl_4 (Pressure Chemical), $Pb(NO_3)_2$ (Strem), and $TlNO_3$ (Strem). $(Ph_3As)_4Pt$, $(dba)_2Pt$,[27] $Pd_2(dba)_3{\cdot}CHCl_3$,[28] and P_2bpy[3,29] were prepared according to literature procedures. P_2phen was originally reported by Ziessel;[3] however, slight modifications were employed and are outlined below in detail. NMR chemical shift reference materials used were the following: ^{205}Tl, $TlNO_3$; ^{195}Pt, H_2PtCl_6 in D_2O; ^{31}P, 85% H_3PO_4. ^1H NMR spectra were internally referenced to residual signal in $CDCl_3$, CD_3CN, CD_3OD, and DMSO-d_6 (as received from Cambridge Isotope Labs). Cyclic voltametric experiments were carried out using a BAS CW50 instrument with the following cell configuration: Pt or glassy carbon working electrodes, Pt wire auxiliary electrode, Ag/AgCl reference in a modified Lugin electrode. Solutions were prepared with 0.1 M TBAP as electrolyte in nitrogen purged MeCN or CH_2Cl_2 and referenced to internal Cp_2Fe (+400 mV). Combustion analysis was carried out by Desert Analytics, Tucson, AZ. UV−visible spectra were obtained using a Hewlett-Packard 8453 diode array spectrometer (1-cm-path length cells). Emission data were recorded using a PTI steady-state fluorometer.

Preparation of 2,9-Bis(diphenylphosphino)-1,10-phenanthroline. A 500-mL flask fitted with a high-efficiency coldfinger, a 125-mL addition funnel, and a two-way gas inlet port was cooled to −78 °C and 80 mL of $NH_{3(l)}$ condensed. Under a nitrogen counter flow, 0.096 g of $Na_{(s)}$ (4.192 mmol) was added. After 15 min, 0.784 g of $HPPh_2$ (4.216 mmol) was added dropwise. After an additional 45 min at −78 °C, 0.500 g of 2,9-dichloro-1,10-phenanthroline[30] (2.00 mmol) (in 60 mL of THF) was added dropwise over a 60-min period. Upon warming to ambient temperature, the reaction was quenched with 5 mL of methanol. Volatiles were then removed in vacuo. The residue was taken up in 50 mL of CH_2Cl_2 and passed through a small pad of Celite. The solvent was removed, and the crude product was crystallized from ethanol, affording the ligand as a white solid, 0.603 g (1.100 mmol, 55%). ^1H NMR (300 MHz, $CDCl_3$, 25 °C): $\delta = 8.027$ (d, $J = 8.0$ Hz, 2H), 7.712 (s, 2H), 7.652 (m, 8H), 7.393 (d, $J = 8.0$ Hz, 2H), 7.304 (m, 12H). $^{13}C\{^1H\}$ NMR (75.5 MHz, $CDCl_3$, 25 °C): $\delta = 137.0$, 135.1, 134.8, 134.5, 129.1, 128.7, 128.6, 127.4, 126.8, 126.5. $^{31}P\{^1H\}$ NMR (121 MHz, $CDCl_3$, external reference H_3PO_4): $\delta = -2.7$ (s).

Preparation of $[Pt_2Tl(P_2phen)_3](NO_3)$, 1. A 500-mL round-bottomed flask was charged with 0.100 g (0.1824 mmol) of 2,9-bis-(diphenylphosphino)-1,10-phenanthroline dissolved in 20 mL of CH_2Cl_2. $Tl(NO_3)$ (0.161 g, 0.606 mmol) dissolved in 45 mL of MeOH was added slowly with swirling. After the mixture was stirred for 10 min, a suspension of 0.172 g of $Pt(Ph_3As)_4$ (0.1216 mmol) in 1:1 MeOH−CH_2Cl_2 (10 mL) was added, affording an orange-colored solution. After the mixture was stirred an additional 60 min, volatiles were removed, and the residue was dissolved in a minimum amount of MeCN. Flash chromatography (alumina), eluting with MeCN affords, an orange solid after MeCN removal. Precipitation of the orange solid by addition of Et_2O to a saturated $CHCl_3$ solution affords 0.091 g (0.0395 mmol) of **1** as a red-orange solid (65%). Elemental analysis. **1**·CH_2Cl_2 ($C_{109}H_{80}Cl_2N_7O_3P_6Pt_2Tl$), calcd: C, 54.8; H, 3.4; N, 4.1. Found: C, 55.38; H, 3.27; N, 3.85. $^1H\{^{31}P\}$ NMR (500 MHz (obs), 202 MHz (dec), $CDCl_3$, 25 °C): $\delta = 5.804$ (t, $J = 7.5$ Hz), 6.095 (t, $J = 7.5$ Hz), 6.529 (d, $J = 7.5$ Hz), 6.897 (t, $J = 7.5$ Hz), 7.123 (d, $J = 6.0$ Hz), 7.239 (t, $J = 7.5$ Hz), 7.393 (d, $J = 8.0$ Hz), 7.771 (s), 7.971 (d, $J = 8.0$ Hz). $^{31}P\{^1H\}$ NMR (121 MHz, $CDCl_3$, 25 °C): δ 46.1 (s, $^1J(Pt-P) = 4436.6$ Hz). ^{195}Pt NMR (107.0 MHz, DMSO/$CDCl_3$, external reference H_2PtCl_6 in D_2O, 25 °C): $\delta = -4119$ (dq, $^1J(P-Pt) = 4436.6$ Hz, $^1J(^{205}Tl-Pt) = 5560$ Hz). ^{205}Tl NMR (288.8 MHz, DMSO, external reference $Tl(NO_3)$, 25 °C): $\delta = 1865.9$ (br m, $^1J(^{205}Tl-Pt) = 5560$ Hz). UV−vis (CH_2Cl_2, 0.00869 mM), λ in nm (ϵ in M^{-1} cm^{-1}): 237 (103 410), 279 (89 208), 293* (64 030), 308* (40 772), 454 (26 476) [* denotes shoulder].

Preparation of $[Pt_2Tl(P_2bpy)_3](NO_3)$, 2. To a 250-mL Schlenk flask charged with 0.5245 g of P_2bpy (1.0 mmol) dissolved in 60.0 mL of CH_2Cl_2 was added 0.1066 g of $TlNO_3$ (0.40 mmol, 10-mL suspension in MeOH). The mixture was stirred for several minutes and then degassed. To this was added 0.2462 g of $Pt(dba)_2$ (0.0371 mmol) as a 35-mL CH_2Cl_2 solution. The reaction was stirred for 30 min at room temperature, after which it was brought to reflux for 12 h under nitrogen atmosphere. The resulting mixture was passed through Celite, and the solvents were removed. Flash chromatography (neutral alumina) eluting with acetonitrile followed by precipitation with diethyl ether affords 0.0248 g (0.111 mmol, 60%) of a dark red solid. $^1H\{^{31}P\}$ NMR (500 MHz (obs), 202 MHz (dec), $CDCl_3$, 25 °C): $\delta = 6.205$ (t, $J = 8.0$ Hz), 6.535 (t, $J = 7.0$ Hz), 6.693 (d, $J = 7.0$ Hz), 6.817 (t, $J = 8.0$ Hz), 7.076 (d, $J = 7.5$ Hz), 7.139 (t, $J = 7.5$ Hz), 7.173 (d, $J = 7.0$ Hz), 7.602 (t, $J = 7.0$ Hz), 7.727 (d, $J = 8.0$ Hz). $^{31}P\{^1H\}$ NMR (121 MHz, $CDCl_3$, 25 °C): $\delta = 35.3$ (s, $^1J(Pt-P) = 4332$ Hz). ^{205}Tl NMR (288.8 MHz, DMSO, external reference $Tl(NO_3)$, 25 °C): $\delta = 2389.5$ (br m, $^1J(^{205}Tl-Pt) = 6100$ Hz). ^{195}Pt NMR (107.0 MHz, DMSO/$CDCl_3$, external reference H_2PtCl_6 in D_2O, 25 °C): $\delta = -4120$ (dq, $^1J(P-Pt) = 4379$ Hz, $^1J(Tl-Pt) = 6100$ Hz). UV−vis (CH_2Cl_2, 0.007404 mM), λ in nm (ϵ in M^{-1} cm^{-1}): 230 (91 501), 285 (50 703), 469 (20 071).

Preparation of $[Pd_2Tl(P_2phen)_3](NO_3)$, 3. A 100-mL Schlenk flask was charged with 0.200 g (0.3648 mmol) of 2,9-bis(diphenylphosphino)-1,10-phenanthroline dissolved in 10 mL of CH_2Cl_2. To this solution was added 0.324 g (1.216 mmol) of $TlNO_3$ dissolved in 5 mL of 1:1 MeOH/DMSO with stirring. After 10 min the vessel was capped, and the contents were subjected to two freeze−pump−thaw cycles and moved to a glovebox. A suspension of 0.126 g of $Pd_2(dba)_3{\cdot}CHCl_3$ (0.1216 mmol) in MeCN (10 mL) was added dropwise, affording an orange solution. After the mixture was stirred an additional 30 min, volatiles were removed and the residue was dissolved in a minimum amount of MeCN. Flash chromatography (alumina) eluting with MeCN affords an orange solid after MeCN removal. Removal of trace DMSO is accomplished by precipitation of the orange solid by addition of Et_2O to a saturated CH_2Cl_2 solution, affording 0.164 g (0.0785 mmol) of **3** as an orange solid (64%). Elemental analysis. **3**·CH_2Cl_2 ($C_{109}H_{80}Cl_2N_7O_3P_6Pd_2Tl$) calcd: C, 59.2; H, 3.6; N, 4.4. Found: C, 59.66; H, 3.43; N, 4.78. $^1H\{^{31}P\}$ NMR (500 MHz, $CDCl_3$, 25 °C): $\delta = 5.794$ (t, $J = 7.5$ Hz), 6.127 (t, $J = 7.0$ Hz), 6.529 (d, $J = 8.0$ Hz), 6.881 (t, $J = 8.0$ Hz), 7.105 (d, $J = 7.0$ Hz), 7.220 (t, $J = 7.5$ Hz), 7.375 (d, $J = 8.0$ Hz), 7.799 (s), 8.018 (d, $J = 8.0$ Hz). $^{31}P\{^1H\}$ NMR (121 MHz, MeCN/$CDCl_3$, 25 °C): $\delta = 27.12$ (br). ^{205}Tl NMR (288.9 MHz, MeCN, external reference $Tl(NO_3)$, 25 °C): $\delta = 2022.05$ (br). UV−vis (CH_2Cl_2, 0.005176 mM), λ in nm (ϵ in M^{-1} cm^{-1}): 235 (190 586), 281 (167 519), 423 (46 731).

Preparation of $[Pd_2Tl(P_2bpy)_3](NO_3)$, 4. P_2bpy (0.1572 g, 0.3 mmol) was dissolved in 40.0 mL of CH_2Cl_2 and placed in a Schlenk flask. To this was added 10 mL of a methanolic suspension of $TlNO_3$ (0.0267 g, 0.1 mmol). The mixture was degassed and placed inside a drybox. To this was added a 20-mL CH_2Cl_2 solution of $Pd_2dba_3{\cdot}CHCl_3$ (0.1035 g, 0.1 mmol). The reaction was stirred for 30 min, during which time the mixture turned dark. The mixture was passed through Celite, and the solvents were evaporated using a rotary evaporator. Flash chromatography (neutral alumina), eluting with acetonitrile followed by precipitation with diethyl ether, affords 0.0123 g (0.060 mmol, 60%) of a dark red solid. $^{31}P\{^1H\}$ NMR (121 MHz, MeCN/$CDCl_3$, 25 °C): $\delta = 21.6$ (br). ^{205}Tl NMR (288.9 MHz, MeCN, external reference Tl-

(27) Cherwinski, W. J.; Johnson, B. F. G.; Lewis, J. *J. Chem. Soc., Dalton Trans.* **1974**, 1405.

(28) Ukai, T.; Kawazura, H.; Ishii, Y.; Bonnet, J. J.; Ibers J. A. *J. Organomet. Chem.* **1974**, *65*, 253.

(29) Newkome, G. R.; Hager, D. C. *J. Org. Chem.* **1978**, *43*, 947.

(30) (a) Halcrow B. E.; Kermack, W. O. *J. Chem. Soc.* **1946**, 155. (b) Ogawa, S.; Yamaguchi, T.; Gotoh, N. *J. Chem. Soc., Perkin Trans. 1* **1974**, 976.

Table 3. Crystallographic Data for **1**−**4**

	1	**2**	**3**	**4**
formula	$C_{109.25}H_{63}Cl_{0.75}N_7O_5P_6Pt_2Tl$	$C_{126}H_{78}N_7O_7P_6Pt_2Tl$	$C_{132}H_{78}N_7O_3P_6Pd_2Tl$	$C_{126}H_{78}N_7O_7P_6Pd_2Tl$
fw	2360.62	2582.32	2413.00	2404.94
a, Å	33.6379(5)	19.3694(1)	21.1124(8)	19.3452(2)
b, Å	14.81300(10)	19.3694(1)	20.3657(8)	19.3452(2)
c, Å	41.9035(6)	51.9258(2)	26.3042(10)	51.7853(8)
α, deg	90	90	90	90
β, deg	107.7430(10)	90	102.57	90
γ, deg	90	120	90	120
V, Å^3	19886.4(4)	16871.20(14)	11039.1(7)	15785.2(2)
space group	*C*2/*c*	$R\bar{3}c$	*C*2/*c*	$R\bar{3}c$
Z	8	6	4	6
D_{calc}, g/cm^3	1.577	1.525	1.452	1.420
crystal size, mm	0.22 × 0.18 × 0.16	0.24 × 0.23 × 0.20	0.44 × 0.07 × 0.07	0.24 × 0.15 × 0.14
μ(Mo Kα), mm^{-1}	4.597	4.055	1.923	1.890
λ, Å	0.71073	0.71073	0.71073	0.71073
temp, K	138(2)	138(2)	138(2)	138(2)
transm factors	0.82−0.92	0.51−0.44	0.89−0.49	0.80−0.68
R_1, wR_2 ($I > 2\sigma(I)$)	0.0642, 0.1339	0.0436, 0.1312	0.0669, 0.1820	0.0816, 0.2356

(NO_3), 25 °C): $\delta = 2636.7$ (br). UV−vis (CH_2Cl_2, 0.00975 mM), λ in nm (ϵ in M^{-1} cm^{-1}): 301* (67 900), 324 (73 465), 450 (16 653) (* denotes shoulder).

X-ray Crystallography. Crystals of **1**−**4** were grown by slow diffusion of benzene or *n*-Bu_2O into concentrated 1,2-dichloroethane solutions. Suitable crystals were coated with light petroleum oil, mounted on a glass fiber, and placed in the −135 °C nitrogen cold stream of a Siemens SMART diffractometer. Unit cell parameters were determined by least-squares analysis of 5332 reflections with 1.51−θ−22.5° for **1**, 8192 reflections with 1.45−θ−30.0° for **2**, 8019 reflections with 1.50−θ−25.0° for **3**, and 7529 reflections with 1.45−θ−30.0° for **4**. A total of 47 076 reflections were collected in the range $1.51 < \theta < 22.50°$, yielding 12 965 unique reflections ($R_{int} = 0.1533$) for **1**, while a total of 12 495 reflections were collected in the range $1.45 < \theta < 30°$, yielding 5460 unique reflections ($R_{int} = 0.057$) for **2**. A total of 34 122 reflections were collected in the range $1.50 < \theta < 25.00°$, yielding 9727 unique reflections ($R_{int} = 0.0934$) for **3**, while a total of 49 051 reflections were collected in the range $1.45 < \theta < 30°$, yielding 5473 unique reflections ($R_{int} = 0.069$) for **4**.

The data were corrected for Lorentz and polarization effects. Crystal data are given in Table 3. Scattering factors and corrections for anomalous dispersion were taken from a standard source.[31]

Calculations were performed using the Siemens SHELXTL Version 5.10 system of programs refining on F^2. The structures were solved by direct methods. Complex **1** crystallizes in the monoclinic space group *C*2/*c*, with the cation, a nitrate anion disordered over three positions, one water, one methanol solvate, and one-quarter of a dichloromethane which is partially disordered. There is no unusual contact between these moieties. Compounds **2** and **4** are isostructural and crystallize in the rhombohedral space group $R\bar{3}c$. The asymmetric unit of each contains one-sixth of the cation and nitrate anion, two-thirds of a benzene, and two-thirds of a water solvate. Compound **3** crystallizes in the monoclinic space group *C*2/*c*, with one-half of the cation and anion in the asymmetric unit along with one-half of a benzene solvate. The refinement of these data was unremarkable. Simple models of the disorder provided satisfactory refinements.

(31) *International Tables for X-ray Crystallography*: Kynoch Press: Birmingham, England, 1974; Vol. 4.

Acknowledgment is made to the National Science Foundation (CHE-9624281), to the donors of the Petroleum Research Fund, administered by the American Chemical Society, for their generous financial support of this research, and to Mr. Lewis Cary and to Prof. J. H. Nelson for their assistance with the NMR spectroscopy.

Supporting Information Available: Complete table of X-ray crystallographic data and mass spectra plots for **1** and **3** (PDF). X-ray crystallographic data, in CIF format, are also available.This material is available free of charge via the Internet at http://pubs.acs.org.

JA001672S